International Journal of Pharmaceutics 690 (2026) 126541

Contents lists available at ScienceDirect

International Journal of Pharmaceutics

journal homepage: www.elsevier.com/locate/ijpharm

Fabrication and characterization of taste-masked core-shell nanofibre mats for dual drug delivery of antihypertensives in pediatrics

Uloma N. Ubani-Ukoma [a,*,1], Xiunan Li [a], Mahmood Faiyaz [a], Maryam Parhizkar [a], Duncan Q.M. Craig [b], Hend E. Abdelhakim [c]

[a] School of Pharmacy, University College London (UCL), 29-39 Brunswick Square, WC1N 1AX London, United Kingdom
[b] Faculty of Science, University of Bath, Bath BA2 7AY, United Kingdom
[c] Global Business School for Health, UCL, 7 Sidings St, E20 2AE London, United Kingdom

ARTICLE INFO

Keywords:
Pediatrics
Taste-masking
Electrospinning
Fixed-dose combination
Antihypertensives
Nanofibres
Drug adherence

ABSTRACT

Drug adherence in pediatrics can be challenging due to bitter drug taste, dysphagia and polypharmacy. With pediatric hypertension on the rise worldwide, this study investigated the use of electrospinning to create a novel taste-masked, fixed-dose combination of lisinopril dihydrate (LIS) and amlodipine besylate (AML) for paediatric use. Electrospun nanofibres of the antihypertensives were formulated as core–shell fibres with polyvinylpyrrolidone (PVP), and Eudragit® EPO (EEPO) by applying an electrical charge to a viscous mixture of the drugs, polymers and solvents. The drug loading, release kinetics, morphology, thermal analysis, physical and solid-state characterization of the fibre mats were evaluated. Taste-masking was investigated *in vitro* by electronic-tongue analysis. Scanning electron microscopy (SEM) and transmission electron microscopy (TEM) analyses showed smooth, non-beaded core–shell fibres with diameters in the nanorange. Fourier transform infrared (FTIR) spectroscopy and x-ray diffraction (XRD) studies confirmed the drugs were amorphously dispersed within the fibres and thermal analysis studies showed acceptable stability profile of the formulations. Both drugs were over 90 % released in 15 mins consistent with immediate release formulations. The e-tongue mean sensor response plot showed the nanofibre mats achieved a statistically significant enhanced taste-masking ($p < 0.0001$) compared to raw amlodipine which registered a high bitterness reading of 87 mV. This study therefore indicates that coaxial electrospinning may be used to produce a fixed-dose taste masked nanofibre mat of LIS and AML that can potentially be used to improve adherence in children.

1. Introduction

Non-adherence or poor adherence to therapy occurs when a patient does not take medication according to the prescribed dosage regimen (Vrijens et al., 2012); this may result in poor treatment outcomes, drug resistance, complications and financial losses (Muture et al., 2011). Poor adherence is prevalent in both adults and children, although it is more common in pediatrics (Kardas et al., 2021) According to Mcgrady and Hommel, out of approximately 63 % of children and adolescents diagnosed with chronic illnesses, 50 % to 88 % of them are non-adherent to their prescribed medications (McGrady and Hommel, 2013) and this can be attributed to poor tasting drugs, dysphagia and polypharmacy (Bukhary et al., 2018; Uestuener et al., 2014; Chachlioutaki et al., 2020). Children are more sensitive to bitter, sour or aversive tastes, a major deterrent to compliance to therapy (Felton, 2018), therefore, age-appropriate dosage forms are required to encourage adherence in pediatrics (Stojmenovski et al., 2024). Some diseases associated with adults do not have age-appropriate dosage forms available for treatment in children. In such uncommon conditions, children may be prescribed unlicensed medicines or given adult medications for off-label use (Chappell, 2015). These medications are either crushed, broken, mixed with food or reconstituted with sweeteners; these practices are associated with difficulty in breaking, uneven doses, stability issues and loss of drug mass (Poller et al., 2017).

The European Union Paediatric Regulation of 2006 requires that appropriate dosage forms for children be developed without subjecting

* Corresponding author.
E-mail addresses: uubani-ukoma@unilag.edu.ng (U.N. Ubani-Ukoma), li.yuki.xiunan@ucl.ac.uk (X. Li), faiyaz.mahmood.21@ucl.ac.uk (M. Faiyaz), maryam.parhizkar@ucl.ac.uk (M. Parhizkar), dqmc21@bath.ac.uk (D.Q.M. Craig), hend.abdelhakim@ucl.ac.uk (H.E. Abdelhakim).
[1] Department of Pharmaceutics and Pharmaceutical Technology, Faculty of Pharmacy, University of Lagos, Nigeria.

https://doi.org/10.1016/j.ijpharm.2025.126541
Received 2 November 2025; Received in revised form 26 December 2025; Accepted 26 December 2025
Available online 30 December 2025

them to unnecessary clinical trials (European Medicines Agency, 2007; Steiner et al., 2024). Also, the use of animals and humans in research is discouraged where a suitable *in vitro* technique is available especially at the early stage of drug development. Consequently, several studies have employed the electronic tongue as a suitable alternative to *in vivo* studies in investigating the palatability of food and drugs (Abdelhakim et al., 2021; Georgieva et al., 2020; Immohr et al., 2017; Keating et al., 2020; Steiner et al., 2024; Tawfik et al., 2021). The e-tongue assesses the bitterness or aversiveness of a drug when it is subjected to its sensor arrays and resulting data can be interpreted by noting the difference in sensor membrane potential between the values obtained from the reference solution and that from the sample solution.

High blood pressure (HBP) is a major risk factor in cardiovascular and renal diseases, early detection and treatment is necessary to prevent morbidity and mortality (Burrello et al., 2018). It is a chronic health condition that requires daily drug administration with best treatment options involving the use of multiple drugs with different mechanisms of action. Adherence is improved if the medications occur as a fixed-dose combination (FDC). Cardiovascular incidences occur mostly in geriatrics but unfortunately, we now see an increase in HBP in pediatrics (Thomas et al., 2022). Song et al. reported a global increase in paediatric hypertension of 75 % to 79 % from 2000 to 2015 and in 2015 alone, they reported an increase of 4.32 % among 6-year-olds, 3.28 % in 19-year-olds and 7.86 % in children aged 14 years (Song et al., 2019). This trend has been attributed to the increased prevalence of obesity in children (Ashraf et al., 2020; Thomas et al., 2022) and treatment with more than one antihypertensive has been shown to improve blood pressure control (Flynn et al., 2017). In these populations, swallowing difficulties, bitterness of drugs and polypharmacy discourage adherence to therapy (Abdelhakim et al., 2020; Bukhary et al., 2018; Punnapurath et al., 2021; World Health Organization, 2023). There are currently no child-friendly formulations available for the management of this disease in children (Ferrarini et al., 2013; Uestuener et al., 2014) and poor management of childhood hypertension has been observed to be associated with later essential hypertension in adults and persistent cardiovascular events (Song et al., 2019).

Amlodipine besylate (AML) and lisinopril dihydrate (LIS) are two antihypertensives commonly used in the management of paediatric hypertension (Thomas et al., 2022). AML is a calcium channel blocker; its bitter taste poses a challenge in its use in pediatrics (Uestuener et al., 2014). LIS is an angiotensin-converting enzyme inhibitor; it is more palatable (Ferrarini et al., 2013), and has a longer duration of action compared to AML. Though there are no known amlodipine/lisinopril fixed-dose antihypertensive in the market, these can be prescribed together to exert a synergistic blood pressure lowering effect.

Recently, drug delivery using nanofibres has been explored as a unique, innovative and versatile way of administering medicines into the body (Ilomuanya et al., 2023). Nanofibres have a high surface area to volume ratio, high porosity and good mechanical strength (Can Suner et al., 2022; Jiffrin et al., 2022; Gareth et al., 2018) and therefore are suitable carriers for drugs. A wide variety of synthetic and natural polymers can be used to control the release kinetics of incorporated drugs, ensure targeted release of the drug, enhance the drug loading properties of the nanofibres, and improve the palatability of drugs (Dziemidowicz et al., 2021; Grimaudo et al., 2020; Samia et al., 2023; Wildy and Lu, 2023).

Polyvinylpyrrolidone (PVP) is a hydrophilic, generally recognized as safe (GRAS) polymer with very good electrospinning properties (Illangakoon et al., 2014). It has been used together with cyclodextrin to taste-mask bitter drugs (Samprasit et al., 2018) and has also found application in facilitating electrospinning when used in combination with polymers that have poor intrinsic electrospinning properties. Eudragit® EPO (EEPO) is a pH dependent taste-masking polymer; drug release from this carrier polymer is expected to occur at a pH < 5.0. This implies that the incorporated drugs release will be prevented in the salivary fluid pH of 7.4 but will be delayed until the delivery system reaches the acidic environment of the stomach. Here we propose that the combination of PVP and EEPO will have a synergistic effect, resulting in both taste masking of incorporated drugs and suitable electrospinnability.

A limited amount of work on fixed-dose combination involving AML and other hypertensives has been performed. Trenfield et al. investigated the non-destructive methods of assessing the quality of LIS and AML in 3D printlets using NMR spectroscopy (Punnapurath et al., 2021); while this study is mainly focused on quality control it also supports the desirability of a fixed-dose combination of these drugs (Trenfield et al., 2020). Bukhary et al. reported the successful characterization of a fixed-dose combination of AML and valsartan as fast dissolving formulation using monoaxial electrospinning (Bukhary et al., 2018). The authors acknowledged the potential of using the electrospun fibres containing multiple drugs to aid adherence in geriatrics.

Electrospinning has been previously utilized in the taste-masking of bitter drugs (Tawfik et al., 2021; Wu et al., 2015). Abdelhakim et al. reported the effectiveness of Kollicoat® smartseal and Eudragit® EPO polymers in taste-masking chlorpheniramine maleate using coaxial electrospinning (Abdelhakim et al., 2021) while Samprasit et al. investigated the use of PVP and cyclodextrin together to taste mask meloxicam, a bitter tasting, non-steroidal anti-inflammatory drug (Samprasit et al., 2015). In both studies, electrospinning was used to formulate nanofibres containing a single drug.

In this study we investigate the effectiveness of PVP and EEPO polymers in fabricating smooth, non-porous, beadless co-axial fibres to deliver a taste-masked, fixed-dose combination of LIS and AML for treatment of paediatric hypertension. As a stretch objective, it is proposed that nanofibre mats fabricated with taste-masking polymers and the dual drug loading will improve drug adherence in children by targeting adherence issues such as drug bitterness, polypharmacy and swallowability.

2. Materials and methods

2.1. Materials

Eudragit® EPO (EEPO), also known as basic butylated methacrylate copolymer, was donated by Evonik (Darmstadt, Germany), polyvinyl pyrrolidone (PVP, 360,000 MWT) was purchased from Alfa Aesar, MA, USA, lisinopril dihydrate (LIS) from Acros Organics, amlodipine besylate (AML) was purchased from LKT laboratories, MN, USA, 99 % *(v/v)* methanol, 99 % *(v/v)* ethanol, and hydrochloric acid were from Fisher Chemicals (Loughborough, UK). Phosphate buffered saline (PBS) tablets pH 7.4 was purchased from MP Biomedicals (Santa Ana, California, USA) and formvar/carbon 300 mesh (pack of 25) from Agarscientific, UK. Tartaric acid was purchased from Sigma Aldrich (Dorset, UK) and potassium chloride was obtained from Scientific Laboratory Supplies (Nottingham, UK). All solvents used were of analytical grade or HPLC grade.

2.2. Methods

2.2.1. Preparation of electrospinning solutions

Placebo solutions for electrospinning were prepared by dissolving EEPO in absolute ethanol to make 35 % (w/v) EEPO solution. The mixture was magnetically stirred at 300 rpm for 2 h and left to stand overnight before electrospinning. PVP was dissolved in methanol to make 10 % (w/v) PVP. The solution was magnetically stirred for 12 h at 300 rpm to obtain a homogenous polymer solution. The choice of polymer concentrations was informed by a combination of preliminary design of experiment study, preformulation studies and literature search (Utkarsh et al., 2020).

Drug-loaded polymer solutions were obtained as follows. LIS was dissolved in absolute methanol to make a 1 % *(w/v)* solution; PVP was added to the mixture to make 10 % (w/v) PVP solution containing 1 %

lisinopril dihydrate. Polymer solution of 35 % (w/v) EEPO and 1 % (w/v) amlodipine was obtained by first dissolving AML in absolute ethanol and then adding EEPO to make 35 % (w/v) AML loaded EEPO polymer solution. The mixture was stirred for 2 h and left to stand before electrospinning.

2.2.2. Coaxial fibre fabrication

Placebo and drug loaded monoaxial fibres and core–shell fibres were made using a Spraybase® electrospinner (Spraybase, Dublin, Ireland) with a flat metal collector. Electrospinning parameters were set at 1 mL/h flow rate, gap distance of 15 cm between the needle tip and stationary collector and applied voltage of 15 kV. The temperature and humidity at operation were 25 ℃ and 40 – 45 % RH respectively. The individual fibres were collected on a foil wrapped around a stationary metal collector to form a nanofibre mat.

Core-shell fibres were obtained by alternating the drug polymer solutions between the core and the shell using coaxial needle of core 20G (inner diameter 0.603 mm and outer diameter 0.908 mm) and shell 14G (inner diameter 1.6 mm and outer diameter 2.109 mm) (Table 1).

2.2.3. Scanning electron microscopy (SEM)

The surface morphology of the fibres was viewed with the Thermo/FEI Quanta 200F (FEI, USA) SEM. A carbon adhesive tab (Agar Scientific, Stansted, UK) was placed on a metal stub, and the paper seal was removed. Small sections of electrospun fibres mats were cut out together with the foil and placed on the SEM stubs (TAAB Laboratories, Reading, UK). The fibres were sputter coated with gold particles in a Quorum Q150T sputter coater (Quorum Technologies Ltd., East Sussex, UK) for 60 s at a sputter current of 20 mA to make them electrically conductive. The vacuum was vented twice before removing the stubs. The samples were placed on the SEM sample holder and loaded into the SEM for imaging at various magnifications. The diameter and size distribution of the fibres were determined by measuring 100 randomly selected strands using ImageJ software (NIH, Maryland, USA).

2.2.4. Transmission electron microscopy (TEM)

TEM was used to confirm the formation of core–shell fibres. During the electrospinning process, fabricated core–shell fibres were collected on a formvar/copper grid by directly placing the grid under the spinneret for a few seconds. The sample was placed on a specimen holder and inserted into a Phillips/FEI CM 120 BioTwin TEM (FEI Company, Hillsboro, OR, USA) for imaging at 120 kV.

2.2.5. Thermogravimetric analysis (TGA)

TGA was performed with the Discovery thermogravimetric analyser (TA Instruments New Castle, DE, USA). Raw powders of the active pharmaceutical ingredients (APIs), polymers, placebo and drug loaded fibre mats of weight ranging from 2.46 to 3.59 mg were analysed in aluminium pans. A heating rate of 10 ℃/min from 40 to 300 ℃ was employed under a nitrogen gas flow rate of 50 mL/min.

Table 1
Coaxial fibre composition (% values refer to concentration in solution prior to spinning).

Formulation	Drug (core)	Polymer (core)	Drug (shell)	Polymer (shell)
CF1	1 % (w/v) LIS	10 % (w/v) PVP	1 % (w/v) AML	35 % (w/v) EEPO
CF2	1 % (w/v) AML	35 % (w/v) EEPO	1 % (w/v) LIS	10 % (w/v) PVP
CF3	1 %(w/v) LIS and 1 % (w/v) AML	10 % (w/v) PVP	–	35 % (w/v) EEPO

2.2.6. Differential Scanning Calorimetry (DSC)

DSC analysis of the APIs, polymer powders, placebo and drug loaded fibres were obtained using TA Instruments Q2000 calorimeter (TA Instruments, New Castle, DE, USA). The weight of the samples in the Tzero aluminium hermetic lid pan (TA Instruments, New Castle, DE, USA) with manually placed pinholes and the reference pans were noted. The experiment was run by equilibrating at 0 ℃, and temperature ramped up by 2 ℃ /min to 210 ℃ in a nitrogen atmosphere of 50 mL/min flow rate.

2.2.7. X-ray diffraction

The solid characterization of the raw materials and electrospun fibres were determined by using Miniflex 600 benchtop diffractometer (Rigaku, Tokyo, Japan). The samples were placed on aluminium pans and inserted into the machine sample holder. A Cu Kα ($\lambda = 1.5418$ Å) was set at a voltage of 40 mV and current of 15 mA. X-ray diffraction patterns of the samples were recorded using diffraction angle ranging from 3° to 50° at a step size of 0.01° and scan speed of 3°/min. Data was plotted and analysed using OriginPro 2023b (OriginLab Corporation, Northampton, MA, USA).

2.2.8. Fourier transform Infrared spectroscopy (FTIR)

The FTIR spectra of the raw materials, placebo electrospun fibres and drug loaded fibres were determined using Spectrum 100 FT-IR spectrometer (Perkin Elmer, Massachusetts, USA). Background scans were conducted, and measurements were performed with a resolution of 16 cm^{-1} and a duration of 32 scans over a range of 4000 – 650 cm^{-1} at room temperature. Infra-red spectra of samples were plotted and analysed using OriginPro 2023b (OriginLab Corporation, Northampton, MA, USA).

2.2.9. Drug release studies and quantification

Drug release from the nanofibres was investigated using Sciquip mini shaker (SciQuip, Wem, UK). The drug loaded nanofibres of weight approximately 10 mg were immersed in 15 mL PBS, pH 7.4 at 37 ± 0.5 ℃ which mimics the neutral pH of the saliva (Baliga et al., 2013). Aliquots of 1 mL of the release medium were withdrawn at predetermined time intervals and replaced with fresh medium to maintain sink conditions. LIS release analysis was performed using HPLC isocratic elution developed from the combined parameters described by Trendfield et al. and Senkardes et al. (Şenkardeş et al., 2017; Trenfield et al., 2020). The mobile phases comprised of HPLC water (adjusted to pH 3 with 1 to 2 drops of phosphoric acid in 500 mL) as solvent A and methanol as solvent B in the ratio of 30:70. An injection volume of 20 µL, flow rate of 1 mL/min, column temperature of 40 ℃ and maximum pressure of 300 bars were used. A C18 analytical column of specifications 150 × 4.6 mm, 5 µm particle size was used. Standard calibration curve for LIS was prepared with sample concentrations of 50, 100, 150, 200, 250, 300, and 350 µg/mL and UV detection was set at a wavelength of 215 nm. All solvents used were of HPLC grade and all samples were filtered through a 0.45 µm membrane filter (Millipore Ltd, Ireland). AML standard curve was prepared using UV/Visible spectrophotometer at 368 nm wavelength. Concentrations of 5, 10, 15, 20, 25, 30, and 35 µg/mL were used.

Coaxial fibre drug loading was determined by dissolving 10 mg of each of the fibres in 10 mL of 50:50 methanol/water solution to ensure complete dissolution of the drugs and polymers. The mixture was stirred magnetically until the complete dissolution of the fibres. Drug quantification was performed using the HPLC and UV/Visible spectrophotometer. The actual drug loading, theoretical drug loading and encapsulation efficiency were calculated according to the method by Abdelhakim et al. and Hashem et al. (Abdelhakim et al., 2021; Hashem et al., 2022). The equations for calculating the drug loading and encapsulation efficiency are shown below in Eqs. (1), 2 and 3.

$$\text{Theoretical Drug loading } (\%) = \frac{\textit{drug content } \left(\frac{w}{v}\%\right)}{\textit{sum of all polymer and drug content } \left(\frac{w}{v}\%\right)} \times 100 \quad (1)$$

$$\text{Actual Drug loading (DL)} = \frac{\textit{Entrapped drug amount}}{\textit{Weight of fibre}} \quad (2)$$

$$\text{Encapsulation Efficiency } (\%) = \frac{\textit{Amount of drug in Nanofibres}}{\textit{Drug initially added}} \times 100 \quad (3)$$

2.2.10. E-tongue analysis

The e-tongue analysis was performed using the TS-5000Z instrument (Insent Inc., Atsugi-shi, Japan) equipped with four lipid membrane sensors and two reference electrodes (New Food Innovation Ltd, UK). The three bitterness sensors used were BT0- pharmaceutical salt bitterness, AN0- basic bitterness, C00- acidic bitterness and the fourth sensor AE1 representing astringency. The negatively charged membrane sensors (AN0 and BT0) and the positively charged membrane sensors (C00 and AEI) were cleaned with alcohol-based washing solutions before commencement of the measurement cycle to ensure thorough cleaning and therefore, high sensitivity of the sensors to the sample solutions. The reference solution was prepared by dissolving 30 mM of KCl and 0.3 mM of tartaric acid in 1L of distilled water. The negatively charged washing solution was prepared by diluting absolute ethanol to 30 % (w/v) with distilled water and adding 100 mM of hydrochloric acid while for the positively charged washing solution, 100 mM of potassium chloride and 10 mM potassium hydroxide were added to the aqueous ethanolic solution.

Each taste analysis cycle consisted of recording the reference potential (V_r) in a reference solution, followed by measuring the electric potential (V_s) in a sample solution for 30 s, after which the sensors were lightly rinsed for 3 s. A third measurement of electric potential (V_{r1}) in a reference solution gives the aftertaste (CPA) followed by a final cleaning process for 330 s (Steiner et al., 2024). Each sample was measured four times and the first measurement discarded to allow for the conditioning of the sensors as recommended by the supplier.

The dose response curves of AML and LIS to the different membrane sensors were plotted to determine their sensitivity to the different taste sensors.

The bitterness of the raw drugs was analysed and compared to that of the fabricated core–shell fibres using the AN0 membrane sensor for basic bitterness, the C00 membrane sensor for acidic bitterness and AE1 for astringency. Freshly fabricated core–shell fibres were made with EEPO and PVP (1,300, 000 MWT) for the e-tongue analysis. Fabricated nanofibres of weight 352.5 mg, equivalent to a selected clinical dose of 1.5 mg/5 mL in 50 mL (10 doses) for both AML and LIS, were utilised in the e-tongue assessment. The dose of 1.5 mg/5 mL for each of the drugs was selected based on the average weight of a 6-year-old with a clinical dose of 0.7 mg/kg for LIS and 0.1 mg/kg for AML (National Institute for Health and Care Excellence, 2025a, 2025b). The taste masking effect of the formulations were assessed by measuring the difference in electric potential between the taste sensor (V_s) and a reference electrode (V_r).

2.2.11. Statistical analysis

Data are expressed as mean values ± standard deviation. Statistical analysis was performed using Origin pro 2023b (Origin Lab, Northampton, MA, USA) for nanofibre characterization, MS Excel 365 (Microsoft, Redmond, Washington, USA) for drug release kinetics and GraphPad Prism (GraphPad, Boston, Massachusetts, USA) for taste-masking comparison.

3. Results and discussion

3.1. Morphological characterization of monoaxial and coaxial electrospun fibres

3.1.1. Scanning electron microscopy, transmission electron microscopy and fibre diameter distribution

The SEM of drug loaded monoaxial fibres, placebo core–shell fibres and dual drug loaded core–shell fibres (Fig. 1) confirmed the successful formation of the fibres at the onset of fibre fabrication and informed the electrospinning parameters and conditions for the different core–shell fibres.

Monoaxial fibres of LIS in PVP dissolved in methanol and monoaxial fibres of AML in ethanol showed well arranged, smooth and beadless fibres. Dual drug loading by co-axial electrospinning resulted in the modification of the electrospinning parameters to get good fibres. Though the feed rate of the different solvent systems and the gap distance between the needle tip and the collector remained the same, the voltage was increased from 12 – 15 kV for the monoaxial fibres and to between 15 – 20 kV for the core–shell fibres. This change in voltage was necessary to overcome the surface tension of the two polymer solutions as they were pumped out from the spinneret during coaxial electrospinning.

All the coaxial drug-loaded fibres had a mean diameter in the nanorange – 265 ± 160 nm, 358 ± 228 nm and 246 ± 183 nm for CF1 (LIS & PVP core and AML & EEPO shell), CF2 (AML & EEPO core and LIS & PVP shell) and CF3 (LIS, AML & PVP core and EEPO shell) respectively (Fig. 2). Fibre diameters in the nanorange increase the surface area of the formulation which will result in faster dissolution and release of the drugs. In contrast, the coaxial placebo fibres had a much higher average diameter of 1159 ± 484 nm. This difference in diameter between the drug loaded and the placebo fibres may be attributed to the presence of the salt forms of the drugs or a reduction in viscosity of the polymer-drug-solvent mixture which enhances the electrospinning process resulting in finer fibres. The CF2 nanofibres exhibited a bimodal distribution possibly due to the presence of a few beads.

This could be attributed to the electrospinning of the PVP/lisinopril combination on the shell with an increased needle size of 14G and the low viscosity of the PVP-lisinopril-methanol mixture. Studies have shown that larger needle diameters produce thicker fibres, affect the solution's viscosity and increase the chance of bead formation during electrospinning (Abunahel and Azman, 2018; He et al., 2019). Beads are undesirable because it affects the release behaviour of incorporated drugs and therefore reproducibility of the fabricated fibres (Kielholz et al., 2022). Electrospinning of the CF2 Fibres with a higher molecular weight PVP (1,300,000) resulted in smooth well aligned beadless fibres.

3.2. Thermal analysis

3.2.1. Thermogravimetric analysis

The TGA thermogram of LIS shows a two-step water loss during heating (Fig. 3) which resulted to a weight loss of 7.15 %. The weight remained constant from 78.00 ℃ until decomposition of LIS started at temperature of 176.11 ℃. The PVP thermogram indicates a loss of water that started from 45.02 ℃ and continued to 73.33 ℃ before stabilizing. The coaxial drug-loaded and placebo fibres show a slight water loss that blends the characteristics of its component polymers – PVP and EEPO. AML decomposition onset occurred at 200.31 ℃. All materials remained stable with increasing temperature except the pure LIS and PVP that exhibited characteristic weight change due to loss of water content. However, within the drug-loaded and placebo core–shell fibres, these weight changes were significantly reduced as observed in the thermogram (Fig. 4).

The percentage weight loss of the drug-loaded CFs at 61.55 ℃ (0.948 %) is less than that of the placebo CFs (2.294 %) (Fig. 4). This could be explained by the presence of the drugs which could have added

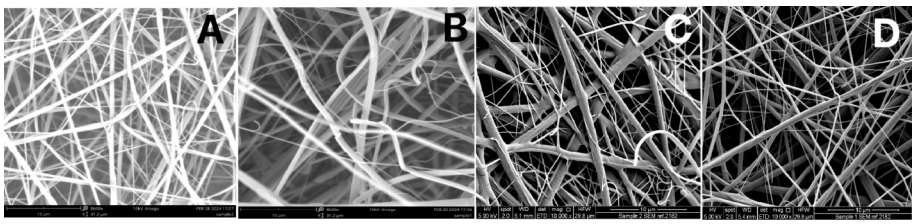

Fig. 1. Scanning electron microscopy (A.) 10% *(w/v)* PVP & 1% *(w/v)* LIS in Methanol monoaxial fibre (B) 35% *(w/v)* EEPO & 1% *(w/v)* AML in Ethanol monoaxial fibre (C) LIS and AML drug loaded fibre (D) Coaxial placebo fibre.

their own weight to the fibres. Consequently, it is possible that the weight loss difference is not significant as this could have been masked by the additional weight of the drugs to the fibres.

3.2.2. *Differential scanning calorimetry*

LIS DSC thermogram show three endothermic peaks at 75 ℃, 101 ℃ and 169 ℃ (Fig. 5). The first two transition temperatures represent the loss of the first and second water molecule in the dihydrate. The weight change then remained constant till a temperature of about 170 ℃ after which melting occurs. The above results are similar to that obtained by other authors that studied the thermal characteristics of lisinopril dihydrate (Alagili et al., 2023; Hinojosa-Torres et al., 2008). The broad endothermic peaks observed in the coaxial drug loaded fibres and co-axial placebo fibres are most likely caused by the loss of water molecules from the hygroscopic PVP polymer (Gareth et al., 2018). A sharp melting endothermic peak is observed at 200 ℃ for AML.

The DSC thermograms indicate that both drug-loaded and placebo nanofibres exhibit a glass transition midpoint at approximately 48 ℃. This was not observed in the API graphs confirming the drugs were molecularly dispersed in the fibre. Also, the endothermic peaks observed in the AML and LIS thermograms are absent in the coaxial formulations confirming their amorphous dispersions in the formulations. The presence of the drugs in the amorphous form enhances their solubility and therefore facilitates the immediate release of these drugs from the nanofibres and faster onset of action.

3.3. *Fourier transform infra-red (FTIR) spectroscopy*

The presence of the polymers and drugs in the formulations are confirmed by the FTIR spectra in Fig. 6. The PVP polymer showed characteristic peaks observed at 3432 cm^{-1} (O–H), 2950 cm^{-1} (C–H stretch) 1649 cm^{-1} (C=O) which are in close relation to that observed by Kamble et al. and Hajikhani et al. (Hajikhani et al., 2021; Kamble et al., 2016). Other distinctive peaks were observed at 1461 cm^{-1} which depicts the scissoring of the CH_2 group, 1286 cm^{-1} also reported by Tawfik et al. (Tawfik et al., 2020) indicative of CH_2 wagging, 1018 cm^{-1} observed by Liu et al. (Liu et al., 2021) at 1019 cm^{-1}, and 844 cm^{-1} which represents a C–C chain (Liu et al., 2021; Raimi-Abraham et al., 2014). These similarities to published data confirm the presence of PVP in the fibres.

EEPO polymer showed a strong aromatic C–H stretching band at 2948 cm^{-1}, a characteristic sharp peak was observed at 1723 cm^{-1} close to that seen by Inam et al. at 1721 cm^{-1} depicting C=O bonds (Inam et al., 2022) and 1238 cm^{-1} representing C-O bond ester group and at 1145 cm^{-1} representing C–C stretching bend (Inam et al., 2022).

LIS characteristic peaks were observed at 1544 cm^{-1} representing $^{+}NH_3$ or $^{+}NH_2$ bending, 1343 cm^{-1} and 1201 cm^{-1} are not assigned and 748 cm^{-1} which depicts phenyl out-of-plane bending (Ip et al., 1992).

The IR spectrum of AML shows peaks at 3166 cm^{1}(C–H bond), 2978 cm^{-1}, 1672 cm^{-1}C= O stretch, 1498 cm^{-1}, 1297 cm^{-1}, 1025 $cm^{-1}NH_3$ wagging, 1095 cm^{-1}C-O-C asymetric stretch, 1019 cm^{-1}, 747 cm^{-1} and 685 cm^{-1}N–H vibrations (Bukhary et al., 2018; Nandiyanto et al., 2019, 2023). Clearly, the peaks in the raw drug spectra have been submerged in those of the core–shell fibres.

The core–shell fibres CF1, CF2 and CF3 had very similar spectra (Fig. 6a) confirming the consistence in the functional groups despite the various arrangement of the polymers/drugs at the core or sheath of the fibres. The characteristic peaks of the pure drugs AML and LIS shown in the Fig. 6b could not be observed in the coaxial drug-loaded fibres spectra indicating that the drugs are amorphously dispersed in the nanofibres. The similarity between the drug-loaded core–shell fibres and the placebo fibre confirms this observation.

3.4. *X-ray diffractometric analysis (XRD)*

The XRD pattern of AML (Fig. 7a) shows definitive peaks at 2θ angles 5°, 11°, 25° and 31° while LIS shows sharp reflections at 7°, 12°, 13°, 16°, 22°, 25°, and 30°. The polymers, PVP and EEPO, patterns show broad halos in appearance with no definite peaks. PVP pattern showed two broad peaks at approximately 10° and 23° while EEPO broad peaks appeared close to 8° and 19°. This suggests that the drugs in their pure state are crystalline while the polymers are amorphous. After electrospinning of the drug-polymer solutions, the fibres obtained had a halo appearance for all three co-axial fibres and the observed reflection peaks in the pure drugs disappeared (Fig. 7b). This implies that the drugs are dispersed on a molecular basis within the fibres as observed in the FTIR spectra.

The XRD patterns distinct Bragg reflections of LIS and AML confirm their crystallinity (Fig. 7). The DSC graphs of the raw drugs also confirm their crystallinity prior to electrospinning because of the absence of glass transition. However, after fabrication of the core–shell fibres, we observe the glass transition in the MTDSC graphs of CF1, CF2 and CF3. The TGA analysis of the individual drugs show water loss from both LIS and PVP due to the presence of the dihydrate molecules and hygroscopicity of the materials respectively. The molecular dispersion of drugs within electrospun fibres have been well documented by many authors (Bukhary et al., 2018; Kamble et al., 2016; Liu et al., 2021; Samprasit et al., 2015; Tawfik et al., 2020; Zhao et al., 2021). This change is expected to enhance the solubility of the drugs as well as their bioavailability.

3.5. *Drug release and quantification*

Drug release data show an initial burst release from the fibres which can be explained by the high aqueous solubility of the PVP polymer in the release medium. PVP is chemically inert, soluble in various solvents and is used in masking unpleasant odours and flavours in combination with other polymers (Franco and De Marco, 2020). Its ability to improve the solubility and therefore the bioavailability of poorly water-soluble drugs, good electrospinning properties and pH stability makes it an ideal carrier for LIS. The choice of PVP as a carrier helps incorporate the drug into the electrospun fibre with the added advantage of improving its palatability as a physical barrier to the ingress of saliva (Felton, 2018). The effect of the hydrophilicity and hygroscopicity of PVP can be seen in the fast release of LIS from the fibres (Fig. 8).

The absorption of the solvent led to the swelling of the polymer which resulted in its release within 30 mins with over 90 % release in 15 mins except for CF2 which was 87 % released (Franco and De Marco,

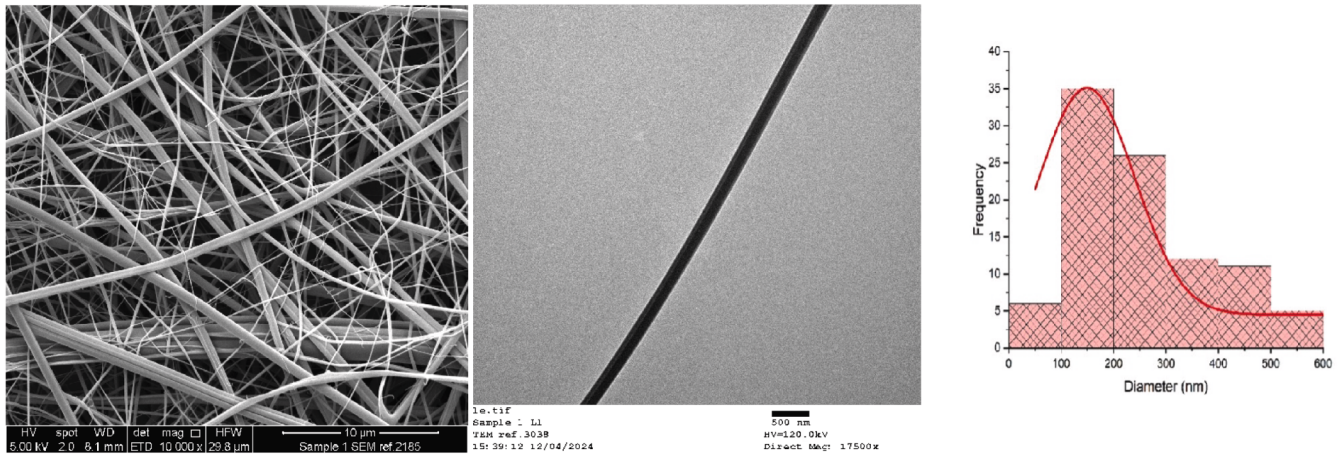

CF2

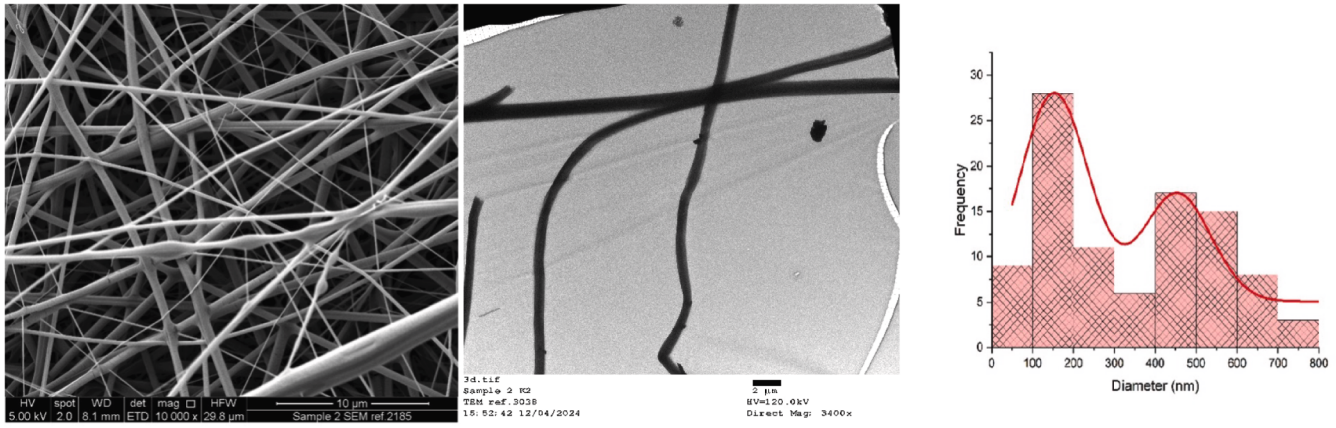

CF3

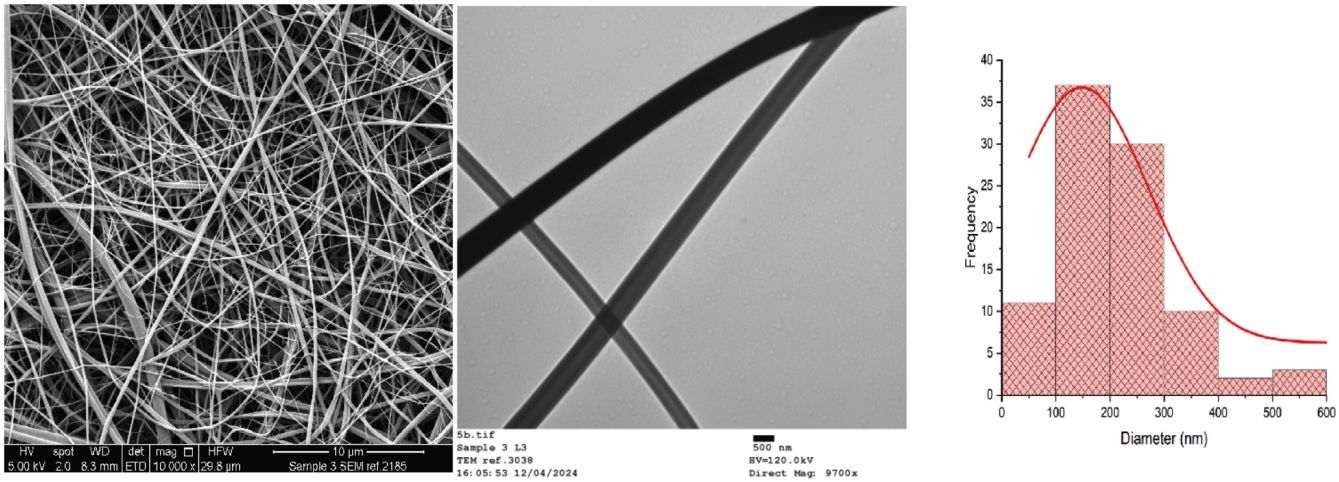

Fig. 2. SEM, TEM and fibre diameter distribution of fabricated core–shell fibres – CF1, CF2 and CF3.

2020). Similarly, Bukhary et al. reported the rapid release of AML and valsartan in less than 5 mins from electrospun fibres formulated with 10 % (w/v) PVP (Bukhary et al., 2018). Eudragit EPO on the other hand is a hydrophobic, pH dependent taste masking polymer (Abdelhakim et al., 2019; Inam et al., 2022). Though not as good as PVP in its spinnability, it ensures the drug release is targeted to the stomach where the pH favours the release of incorporated drugs. EEPO has been utilised as a taste masking polymer, hence its use in this study as a carrier for the bitter antihypertensive, AML. The pH-dependent properties of EEPO are particularly significant during the first 1–2 min of administration when the formulation is still on the tongue, as they help minimize salivary cell sensitivity to the bitter taste of amlodipine. Consequently, the drug release study was conducted in phosphate buffered saline pH 7.4 which mimics the neutral pH of the saliva.

Due to the hydrophobicity of EEPO polymer, the drug release of amlodipine was prolonged to about an hour (100 %) though 90 % of the

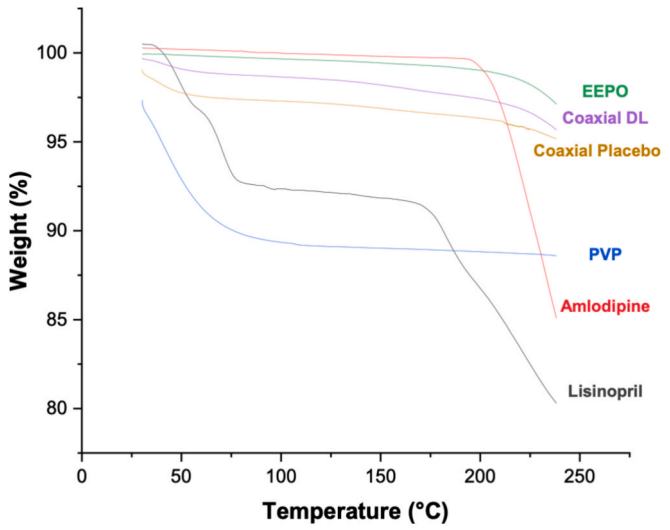

Fig. 3. TGA of polymers, drugs, coaxial placebo and coaxial drug-loaded fibres.

drug was released in 15 mins. Drug release in less than 30 mins ensures rapid onset of action when administered orally. So effectually, the two polymers PVP and EEPO worked together to lead to appropriate release duration expected of oral tablets. Release of the drugs from CF2 had a more sustained release compared to formulations CF1 and CF3. Within 60 s, 27 % LIS was released from CF2 which is significantly different ($p < 0.05$) compared to 52 % from CF1 and 74 % from CF3. In 60 s, AML was 45 % released from CF2 ($p < 0.05$) which is significantly different when compared to 38 % and 69 % respectively from CF1 and CF3. The slower release of the drugs from CF2 could be as a result of the sequestration of the drugs in the beads which led to a partial reduction in burst release (Chen et al., 2023; Zhou et al., 2022). CF3, however, had the fastest release even though the two drugs were incorporated in the core. The fast release could be as a result of the hydrophilic characteristic of PVP coating.

Drug loading and encapsulation studies showed the highest loading for LIS occurred with the CF1 fibres 41.2 ± 1.0 μg/mg while that of AML occurred in the CF2 fibres − 33.0 ± 31 μg/mg. It is observed that these high loading occurred when the drugs were loaded in the core of the fibres compared to the lower loading and encapsulation observed where the drugs are loaded in the shell (Table 2). This is further confirmed by the medial loading and encapsulation efficiency values in the CF3 core–shell fibres where both drugs are encapsulated in the core of the fibres (Table 2). CF3 drug loading for both drugs show an average amount of 35 μg/mg and 20 μg/mg for LIS and AML respectively. Drug loading could be improved by increasing the concentration of the drugs in the electrospinning solution. The EE% is highest for LIS in CF1 at 96 % and highest for AML at 77.4 % in CF2.

Based on the result obtained, it is best to have a hydrophobic polymer at the shell as is with the CF1 and CF3 fibres in cases where coaxial electrospinning is preferred. In addition, the EE% could have been affected by the repeated de-clogging of the needle tip during electrospinning because of the EEPO; this could have resulted in the poor encapsulation observed with the formulations.

3.6. Electronic tongue analysis

The sensor response plots for both drugs at various concentrations across all sensors indicated that AML exhibited both bitterness and astringency, along with a bitter aftertaste (Figs. 9a and b). In contrast, the mean sensor response (MSR) curve of LIS values were within −/+ 5 mV except for the AN0 membrane sensor that is below −5 mV at 10 mM concentration (Figs. 9c and d).

This indicates a poor response of LIS to the sensor membranes. Though the sensor arrays were not sensitive to LIS, this does not constitute a challenge as children generally consider the drug to be palatable (Ferrarini et al., 2013).

The drugs and fabricated fibres were sensitive to the negatively charged membrane sensor AN0 but poorly sensitive to the positively charged membrane sensor C00 which detect basic bitterness and acidic bitterness respectively. The AE1 membrane sensor for astringency was sensitive to AML but had a poor aftertaste response. Therefore, the AN0 sensor was used to assess the bitterness threshold of the taste masked fibres in comparison to the raw drug.

The e-tongue analysis shows successful taste masking of the bitter AML in the formulations particularly for formulation CF2 which had the AML and EEPO at the core and the LIS and PVP on the shell and the CF3 with both drugs at the core with PVP and EEPO on the shell. The negative values of LIS and CF1 observed in the mean sensor response (MSR) plot indicates that these were undetected by the AN0 sensor.

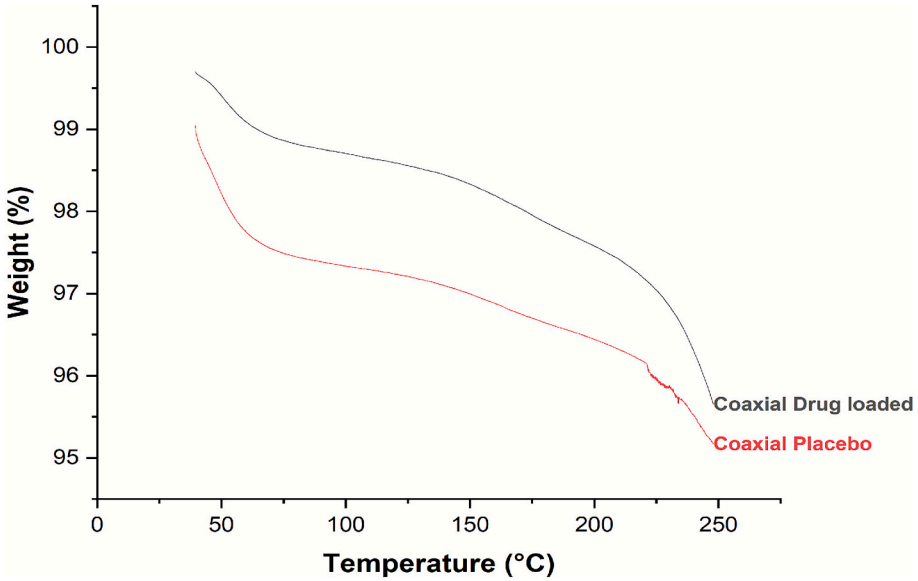

Fig. 4. TGA graph of the coaxial placebo nanofibres and drug loaded nanofibres show a percentage weight loss of 0.948% for the drug loaded nanofibres and 2.294% for the placebo fibres at 61 ℃.

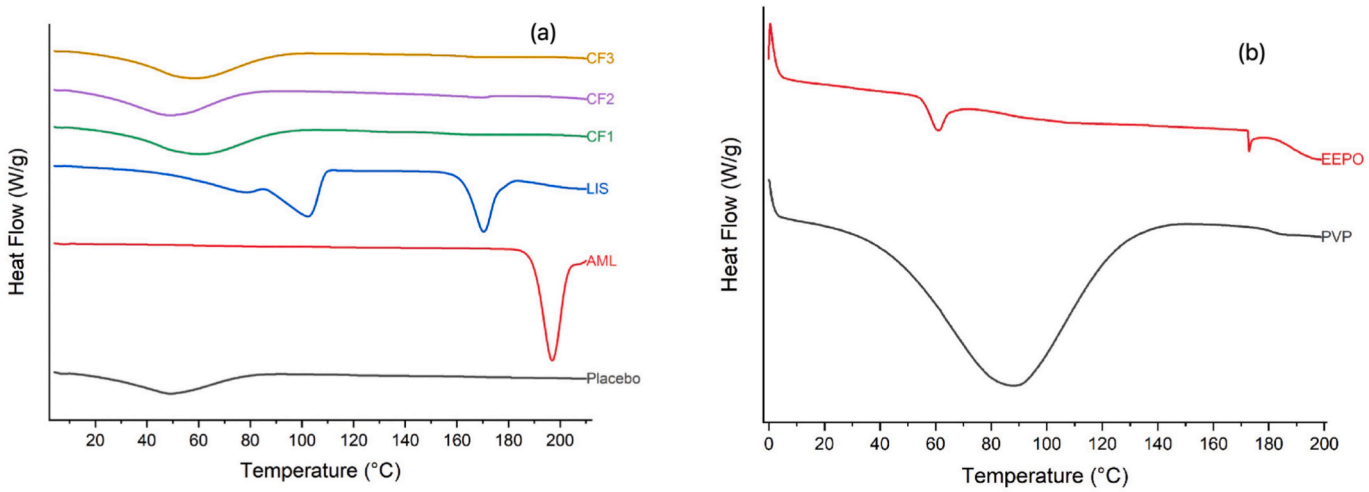

Fig. 5. DSC graph of (a) APIs, drug-loaded core–shell nanofibres and placebo core–shell nanofibres and (b) PVP and EEPO Polymers.

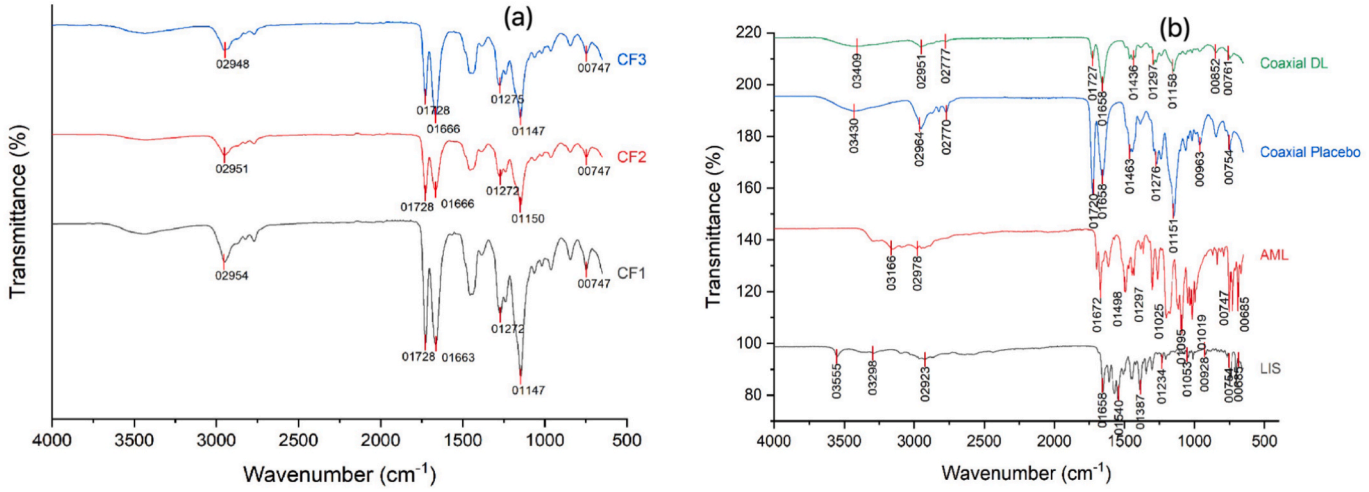

Fig. 6. FTIR spectra (a) core–shell fibres CF1, CF2, and CF3 (b) APIs, coaxial placebo and coaxial drug-loaded.

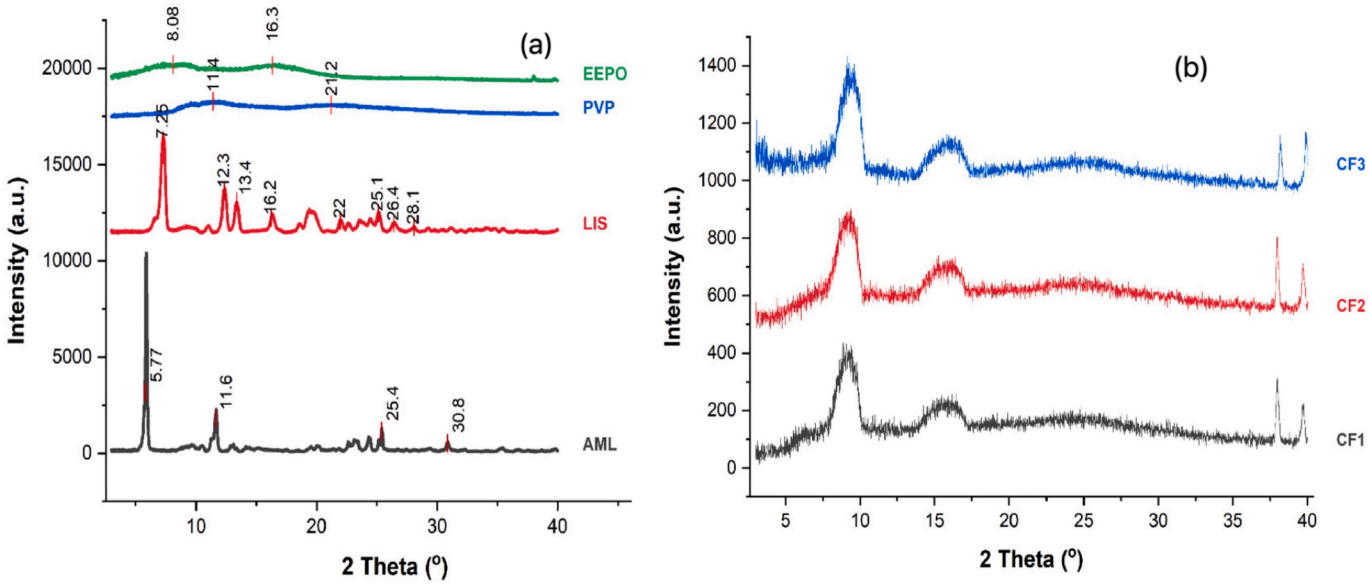

Fig. 7. XRD pattern (a) APIs and polymers (b) Core-shell fibres.

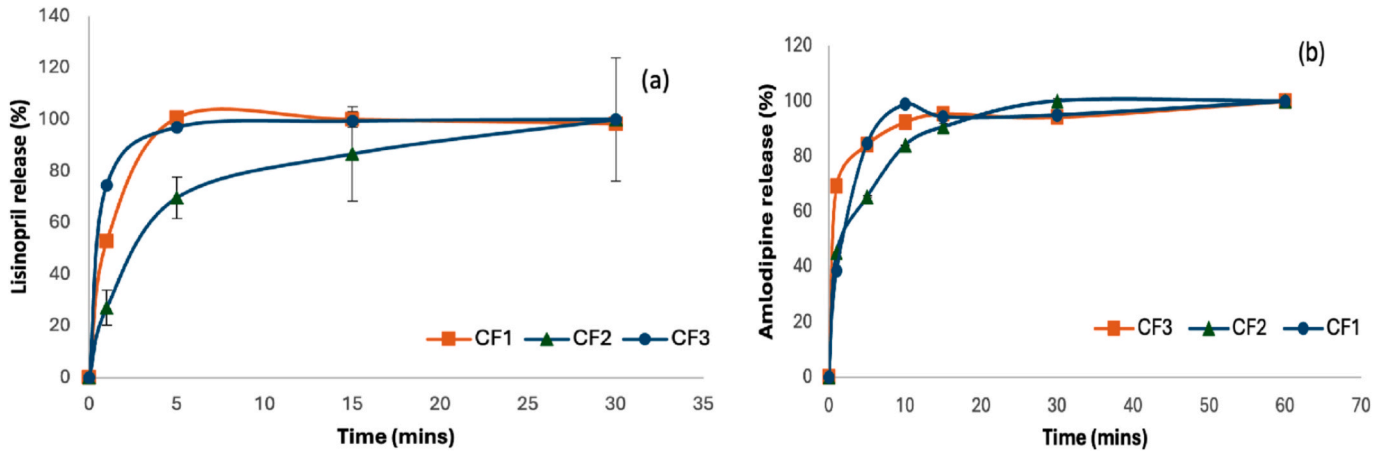

Fig. 8. Drug release profiles of loaded core–shell fibres (a) percentage lisinopril dihydrate release (b) percentage amlodipine besylate release. CF1(LIS & PVP core and AML & EEPO shell), CF2 (AML & EEPO core and LIS & PVP shell) and CF3 (LIS, AML & PVP core and EEPO shell).

Table 2
Drug loading and encapsulation efficiency.

	Lisinopril dihydrate		Amlodipine besylate	
	DL (μg/mg)	EE (%)	DL (μg/mg)	EE (%)*
CF1	41.2 ± 1.0	96.8 ± 2.0	16.3 ± 7	38.2 ± 17
CF2	22.7 ± 0.2	53.4 ± 0.3	33.0 ± 31	77.4 ± 73
CF3	35.0 ± 0.1	82.3 ± 0.2	19.9 ± 6	46.8 ± 13

n = 3, values are in mean ± S.D.

Compared to the formulations, raw AML, the control sample, had a high MSR of 86.9 mV (Fig. 10) which is significantly higher than the MSR of the fabricated taste-masked nanofibres ($p < 0.0001$).

The MSR graph of the AN0 membrane sensor confirms the successful taste masking of all three formulations compared to the amlodipine raw drug. Formulation CF2 had the lowest MSR value 0.31 mV, followed by CF3, 2.36 mV and then CF1 whose bitter taste was undetected. This shows a significant reduction of the drug's bitterness in the core–shell fibres.

4. Conclusion

In this study, we have explored the possibility of using electrospinning to produce a fixed-dose combination of two antihypertensive drugs incorporated in taste masking polymer carriers. The release of these drugs were controlled or modified by using the hydrophilic polymer with excellent spinnability – PVP and a hydrophobic polymer with

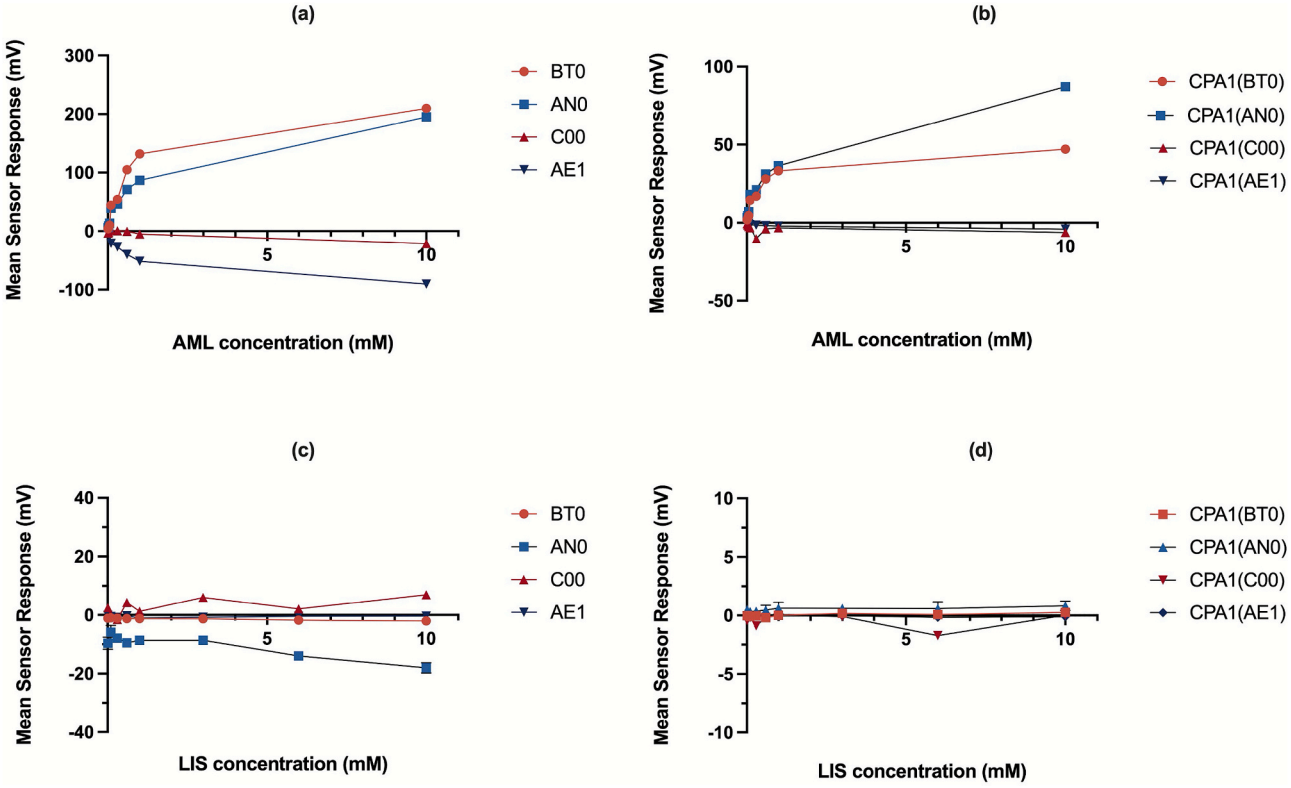

Fig. 9. Analysis of sensor responses to various concentrations of AML and LIS. BT0- pharmaceutical salt bitterness; AN0- basic bitterness; C00- acidic bitterness; AE1- astringency.

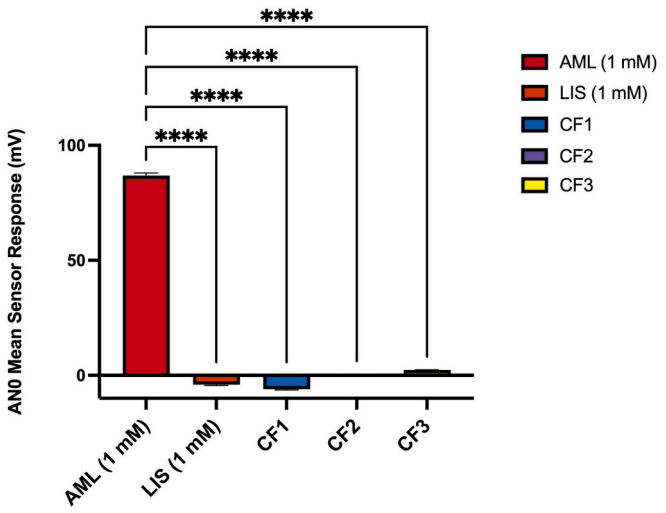

Fig. 10. A bar chart showing the E-tongue response to raw amlodipine and core–shell fibres different formulations, with AN0 as the focused sensor ("****" means $p < 0.0001$).

pH dependent solubility – EEPO. The morphological tests of light microscopy, SEM and TEM confirmed the fabrication of smooth, unbeaded drug-loaded coaxial fibers within the nanorange except for CF2 that is slightly beaded. The thermal properties of the fabricated fibers show good stability over a wide range of temperature as indicated by the DSC and TGA results. The nature and compatibility of the drugs with the polymers confirmed the change of the drugs from crystalline to amorphous in the core–shell fibres using solid characterizations of XRD and FTIR. The drug loading, encapsulation efficiency and release obtained indicated a release highly influenced by the polymer carrier and the position of the polymer-drug solution *in* the core or shell of the fibres and the e-tongue analysis attested to the taste masking effectiveness of the formulations. Electrospun nanofibres may offer significant advantages in the development of paediatric formulations through fixed-dose combinations and taste masking of bitter medications. This will improve palatability and potentially enhance adherence to therapy specifically for long term treatments associated with chronic diseases like hypertension.

The limitations of this study include the low sensitivity of the e-tongue to LIS and the absence of pharmacokinetic studies needed to confirm the safety and efficacy of the selected AML and LIS doses in children, highlighting the need for *in vivo* studies. This, notwithstanding, a good foundation has been laid for future studies on the stability of LIS and AML fixed-dose antihypertensive fabricated nanofibres mats, formulation of the optimized fibres as oral films or minitablets appropriate for pediatrics and *in vivo* studies using human taste panels and/or the brief-access taste aversion (BATA) assay. Further studies will be conducted according to paediatric regulations, providing the basis for a paediatric investigative plan aimed at developing a fixed-dose antihypertensive medicine for children.

CRediT authorship contribution statement

Uloma N. Ubani-Ukoma: Writing – review & editing, Writing – original draft, Visualization, Validation, Methodology, Investigation, Funding acquisition, Formal analysis, Data curation, Conceptualization. **Xiunan Li:** Writing – review & editing, Investigation, Formal analysis, Data curation. **Mahmood Faiyaz:** Writing – review & editing, Validation, Investigation, Formal analysis, Data curation. **Maryam Parhizkar:** Writing – review & editing, Validation, Supervision, Resources, Project administration, Methodology. **Duncan Q.M. Craig:** Writing – review & editing, Validation, Supervision, Project administration, Methodology, Conceptualization. **Hend E. Abdelhakim:** Writing – review & editing, Validation, Supervision, Resources, Project administration, Methodology, Conceptualization.

Funding

This research was funded by the Tertiary Education Trust Fund, Abuja, Nigeria through the University of Lagos, Nigeria with award number – TETF/ES/UNIV/LAGOS/TSAS/2022.

Declaration of competing interest

The authors declare that they have no known competing financial interests or personal relationships that could have appeared to influence the work reported in this paper.

Acknowledgement

The authors acknowledge Dr. Andrew Weston of the School of Pharmacy, University College London, United Kingdom for his assistance with TEM and SEM imaging. Graphical abstract was created with biorender.com.

Data availability

Data will be made available on request.

References

Abdelhakim, H.E., Coupe, A., Tuleu, C., Edirisinghe, M., Craig, D.Q.M., 2021. Utilising co-axial electrospinning as a taste-masking technology for paediatric drug delivery. Pharmaceutics 13. https://doi.org/10.3390/pharmaceutics13101665.

Abdelhakim, H.E., Coupe, A., Tuleu, C., Edirisinghe, M., Craig, D.Q.M., 2019. Electrospinning optimization of eudragit e PO with and without chlorpheniramine maleate using a design of experiment approach. Mol. Pharm. 16, 2557–2568. https://doi.org/10.1021/acs.molpharmaceut.9b00159.

Abdelhakim, H.E., Williams, G.R., Craig, D.Q.M., Orlu, M., Tuleu, C., 2020. Human mouthfeel panel investigating the acceptability of electrospun and solvent cast orodispersible films. Int. J. Pharm. 585, 119532. https://doi.org/10.1016/j.ijpharm.2020.119532.

Abunahel, B.M., Azman, N.N., 2018. Effect of needle diameter on the morphological structure of electrospun n-Bi2O3/epoxy-PVA nanofiber mats 12, 296–299.

Alagili, M.F., AlQuadeib, B.T., Ashri, L.Y., Ibrahim, M.A., 2023. Optimization and evaluation of Lisinopril mucoadhesive sustained release matrix pellets: In-vitro and ex-vivo studies. Saudi Pharmaceut. J. 31. https://doi.org/10.1016/j.jsps.2023.06.023.

Ashraf, M., Irshad, M., Parry, N.A., 2020. Pediatric hypertension: an updated review. Clin. Hypertens. 26, 1–6. https://doi.org/10.1186/s40885-020-00156-w.

Baliga, S., Muglikar, S., Kale, R., 2013. Salivary pH: a diagnostic biomarker. J Indian Soc Periodontol 17, 461–465. https://doi.org/10.4103/0972-124X.118317.

Bukhary, H., Williams, G.R., Orlu, M., 2018. Electrospun fixed dose formulations of amlodipine besylate and valsartan. Int. J. Pharm. 549, 446–455. https://doi.org/10.1016/j.ijpharm.2018.08.008.

Burrello, J., Erhardt, E.M., Saint-Hilary, G., Veglio, F., Rabbia, F., Mulatero, P., Monticone, S., D'Ascenzo, F., 2018. Pharmacological treatment of arterial hypertension in children and adolescents. A network meta-analysis. Am. Heart Assoc. 306–313.

Can Suner, S., Yildirim, Y., Yurt, F., Ozel, D., Oral, A., Ozturk, I., 2022. Antibiotic loaded electrospun poly (lactic acid) nanofiber mats for drug delivery system. J Drug Deliv Sci Technol 71. https://doi.org/10.1016/j.jddst.2022.103263.

Chachlioutaki, K., Tzimtzimis, E.K., Tzetzis, D., Chang, M.W., Ahmad, Z., Karavasili, C., Fatouros, D.G., 2020. Electrospun orodispersible films of isoniazid for pediatric tuberculosis treatment. Pharmaceutics 12. https://doi.org/10.3390/pharmaceutics12050470.

Chappell, F., 2015. Medication adherence in children remains a challenge. Prescriber 26, 31–34. https://doi.org/10.1002/psb.1371.

Chen, W., Zhao, P., Yang, Y., Yu, D.-G., 2023. Electrospun beads-on-the-string nanoproducts: preparation and drug delivery application. Curr. Drug Deliv. 20, 1224–1240. https://doi.org/10.2174/1567201819666220525095844.

Dziemidowicz, K., Sang, Q., Wu, J., Zhang, Z., Zhou, F., Lagaron, J.M., Mo, X., Parker, G. J.M., Yu, D.G., Zhu, L.M., Williams, G.R., 2021. Electrospinning for healthcare: recent advancements. J. Mater. Chem. B 9, 939–951. https://doi.org/10.1039/d0tb02124e.

European Medicines Agency, 2007. Paediatric Regulation [WWW Document]. European Medicines Agency. URL https://www.ema.europa.eu/en/human-regulatory-overview/paediatric-medicines-overview/paediatric-regulation (accessed 9.14.25).

Felton, L.A., 2018. Use of polymers for taste-masking pediatric drug products. Drug Dev. Ind. Pharm. https://doi.org/10.1080/03639045.2018.1430822.

Ferrarini, A., Bianchetti, A.A., Fossali, E.F., Faré, P.B., Simonetti, G.D., Lava, S.A.G., Bianchetti, M.G., 2013. What can we do to make antihypertensive medications taste better for children? Int. J. Pharm. 457, 333–336. https://doi.org/10.1016/j.ijpharm.2013.07.054.

Flynn, J.T., Kaelber, D.C., Baker-Smith, C.M., 2017. Clinical practice guideline for screening and management of high blood pressure in children and adolescents. Pediatrics 140.

Franco, P., De Marco, I., 2020. The use of poly(N-vinyl pyrrolidone) in the delivery of drugs: a review. Polymers (Basel) 12, 18–21. https://doi.org/10.3390/POLYM12051114.

Gareth, W., Raimi-Abraham, B.T., Luo, C.J., 2018. Nanofibres in Drug Delivery, First Edit. ed. UCL Press, London.

Georgieva, Y., Kassarova, M., Kokova, V., Apostolova, E., Pilicheva, B., 2020. Taste masking of enalapril maleate by microencapsulation in Eudragit EPO® microparticles. Pharmazie 75, 61–69. https://doi.org/10.1691/ph.2020.9123.

Grimaudo, M.A., Concheiro, A., Alvarez-Lorenzo, C., 2020. Crosslinked hyaluronan electrospun nanofibers for ferulic acid ocular delivery. Pharmaceutics 12, 1–14. https://doi.org/10.3390/pharmaceutics12030274.

Hajikhani, M., Emam-Djomeh, Z., Askari, G., 2021. Fabrication and characterization of mucoadhesive bioplastic patch via coaxial polylactic acid (PLA) based electrospun nanofibers with antimicrobial and wound healing application. Int. J. Biol. Macromol. 172, 143–153. https://doi.org/10.1016/j.ijbiomac.2021.01.051.

Hashem, H.M., Motawea, A., Kamel, A.H., Bary, E.M.A., Hassan, S.S.M., 2022. Fabrication and characterization of electrospun nanofibers using biocompatible polymers for the sustained release of venlafaxine. Sci. Rep. 12, 18037. https://doi.org/10.1038/s41598-022-22878-7.

He, H., Kara, Y., Molnar, K., 2019. Effect of needle characteristic on fibrous PEO produced by electrospinning. Resolut. Discov. 4, 7–11. https://doi.org/10.1556/2051.2018.00063.

Hinojosa-Torres, J., Aceves-Hernández, J.M., Hinojosa-Torres, J., Paz, M., Castaño, V.M., Agacino-Valdés, E., 2008. Degradation of lisinopril: a physico-chemical study. J. Mol. Struct. 886, 51–58. https://doi.org/10.1016/j.molstruc.2007.03.064.

Illangakoon, U.E., Gill, H., Shearman, G.C., Parhizkar, M., Mahalingam, S., Chatterton, N.P., Williams, G.R., 2014. Fast dissolving paracetamol/caffeine nanofibers prepared by electrospinning. Int. J. Pharm. 477, 369–379. https://doi.org/10.1016/j.ijpharm.2014.10.036.

Ilomuanya, M.O., Bassey, P.O., Ogundemuren, D.A., Ubani-Ukoma, U.N., Tsamis, A., Fan, Y., Michalakis, K., Angsantikul, P., Usman, A., Amenaghawon, A.N., 2023. Development of mucoadhesive electrospun scaffolds for intravaginal delivery of Lactobacilli spp., a tenside, and metronidazole for the management of bacterial vaginosis. Pharmaceutics 15. https://doi.org/10.3390/pharmaceutics15041263.

Immohr, L.I., Dischinger, A., Kühl, P., Kletzl, H., Sturm, S., Günther, A., Pein-Hackelbusch, M., 2017. Early pediatric formulation development with new chemical entities: Opportunities of e-tongue besides human taste assessment. Int. J. Pharm. 530, 201–212. https://doi.org/10.1016/j.ijpharm.2017.07.069.

Inam, S., Irfan, M., Lali, N.U.A., Syed, H.K., Asghar, S., Khan, I.U., Khan, S.U.D., Iqbal, M. S., Zaheer, I., Khames, A., Abou-Taleb, H.A., Abourehab, M.A.S., 2022. Development and characterization of Eudragit® EPO-based solid dispersion of rosuvastatin calcium to foresee the impact on solubility, dissolution and antihyperlipidemic activity. Pharmaceuticals 15. https://doi.org/10.3390/ph15040492.

Ip, D.P., DeMarco, J.D., Brooks, M.A., 1992. Analytical profiles of drug substances - Lisinopril. Academic Press, Inc. DOI: 10.1016/S0065-2377(08)60212-4.

Jiffrin, R., Razak, S.I.A., Jamaludin, M.I., Hamzah, A.S.A., Mazian, M.A., Jaya, M.A.T., Nasrullah, M.Z., Majrashi, M., Theyab, A., Aldarmahi, A.A., Awan, Z., Abdel-Daim, M.M., Azad, A.K., 2022. Electrospun nanofiber composites for drug delivery: a review on current progresses. Polymers (Basel). https://doi.org/10.3390/polym14183725.

Kamble, R.N., Gaikwad, S., Maske, A., Patil, S.S., 2016. Fabrication of electrospun nanofibres of BCS II drug for enhanced dissolution and permeation across skin. J. Adv. Res. 7, 483–489. https://doi.org/10.1016/j.jare.2016.03.009.

Kardas, P., Dabrowa, M., Witkowski, K., 2021. Adherence to treatment in paediatric patients – results of the nationwide survey in Poland. BMC Pediatr. 21, 1–12. https://doi.org/10.1186/s12887-020-02477-z.

Keating, A.V., Soto, J., Forbes, C., Zhao, M., Craig, D.Q.M., Tuleu, C., 2020. Multi-methodological quantitative taste assessment of anti-tuberculosis drugs to support the development of palatable paediatric dosage forms. Pharmaceutics 12, 1–20. https://doi.org/10.3390/pharmaceutics12040369.

Kielholz, T., Walther, M., Jung, N., Windbergs, M., 2022. Electrospun fibers loaded with antimicrobial peptides for treatment of wound infections. Eur. J. Pharm. Biopharm. 179, 246–255. https://doi.org/10.1016/j.ejpb.2022.09.014.

Liu, Y., Li, C., Chen, J., Han, Y., Wei, M., Liu, J., Yu, X., Li, F., Hu, P., Fu, L., Liu, Y., 2021. Electrospun high bioavailable rifampicin–isoniazid-polyvinylpyrrolidone fiber membranes. Appl. Nanosci. (Switzerland) 11, 2271–2280. https://doi.org/10.1007/s13204-021-01957-7.

McGrady, M.E., Hommel, K.A., 2013. Medication adherence and health care utilization in pediatric chronic illness: a systematic review. Pediatrics. https://doi.org/10.1542/peds.2013-1451.

Muture, B.N., Keraka, M.N., Kimuu, P.K., Kabiru, E.W., Ombeka, V.O., Oguya, F., 2011. Nonadherence in tuberculosis treatment: Predictors and consequences in New York City. Am. J. Med. 11, 2–10. https://doi.org/10.1016/S0002-9343(96)00402-0.

Nandiyanto, A.B.D., Oktiani, R., Ragadhita, R., 2019. How to read and interpret ftir spectroscope of organic material. Ind. J. Sci. Technol. 4, 97–118. https://doi.org/10.17509/ijost.v4i1.15806.

Nandiyanto, A.B.D., Ragadhita, R., Fiandini, M., 2023. Interpretation of Fourier transform infrared spectra (FTIR): a practical approach in the polymer/plastic thermal decomposition. Indonesian J. Sci. Technol. 8, 113–126. https://doi.org/10.17509/ijost.v8i1.53297.

National Institute for Health and Care Excellence, 2025a. Lisinopril [WWW Document]. British National Formulary for Children. URL https://bnfc.nice.org.uk/drugs/lisinopril/ (accessed 1.22.25).

National Institute for Health and Care Excellence, 2025b. Amlodipine [WWW Document]. British National Formulary Children. URL https://bnfc.nice.org.uk/drugs/amlodipine (accessed 1.22.25).

Poller, B., Strachan, C., Broadbent, R., Walker, G.F., 2017. A minitablet formulation made from electrospun nanofibers. Eur. J. Pharm. Biopharm. 114, 213–220. https://doi.org/10.1016/j.ejpb.2017.01.022.

Punnapurath, S., Vijayakumar, P., Platty, P., Krishna, S., Thomas, T., 2021. A study of medication compliance in geriatric patients with chronic illness. J. Family Med. Prim Care 10, 1644. https://doi.org/10.4103/jfmpc.jfmpc_1302_20.

Raimi-Abraham, B.T., Mahalingam, S., Edirisinghe, M., Craig, D.Q.M., 2014. Generation of poly(N-vinylpyrrolidone) nanofibres using pressurised gyration. Mater. Sci. Eng. C 39, 168–176. https://doi.org/10.1016/j.msec.2014.02.016.

Samia, F., Conway, B.R., Ghori, M.U., 2023. Nanofibres in Drug Delivery Applications. Fibers 11, 1–37. https://doi.org/10.3390/fib11020021.

Samprasit, W., Akkaramongkolporn, P., Kaomongkolgit, R., Opanasopit, P., 2018. Cyclodextrin-based oral dissolving films formulation of taste-masked meloxicam. Pharm. Dev. Technol. 23, 530–539. https://doi.org/10.1080/10837450.2017.1401636.

Samprasit, W., Akkaramongkolporn, P., Ngawhirunpat, T., Rojanarata, T., Kaomongkolgit, R., Opanasopit, P., 2015. Fast releasing oral electrospun PVP/CD nanofiber mats of taste-masked meloxicam. Int. J. Pharm. 487, 213–222. https://doi.org/10.1016/j.ijpharm.2015.04.044.

Şenkardeş, S., Özaydın, T., Uğurlu, T., Küçükgüzel, G., 2017. Development and validation of a reversed-phase HPLC method for the determination of lisinopril and gliclazide in pharmaceuticals. Marmara Pharm J 21. https://doi.org/10.12991/marupj.300842.

Song, P., Zhang, Y., Yu, J., Zha, M., Zhu, Y., Rahimi, K., Rudan, I., 2019. Global prevalence of hypertension in children: a systematic review and meta-analysis. JAMA Pediatr. 173, 1154–1163. https://doi.org/10.1001/jamapediatrics.2019.3310.

Steiner, D., Meyer, A., Immohr, L.I., Pein-Hackelbusch, M., 2024. Critical View on the qualification of electronic tongues regarding their performance in the development of Peroral drug formulations with bitter ingredients. Pharmaceutics 16. https://doi.org/10.3390/pharmaceutics16050658.

Stojmenovski, A., Gatarić, B., Vučen, S., Railić, M., Krstonošić, V., Kukobat, R., Mirjanić, M., Škrbić, R., Račić, A., 2024. Formulation and evaluation of polysaccharide microparticles for the controlled release of propranolol hydrochloride. Pharmaceutics 16. https://doi.org/10.3390/pharmaceutics16060788.

Tawfik, E.A., Craig, D.Q.M., Barker, S.A., 2020. Dual drug-loaded coaxial nanofibers for the treatment of corneal abrasion. Int. J. Pharm. 581, 119296. https://doi.org/10.1016/j.ijpharm.2020.119296.

Tawfik, E.A., Scarpa, M., Abdelhakim, H.E., Bukhary, H.A., Craig, D.Q.M., Barker, S.A., Orlu, M., 2021. A potential alternative orodispersible formulation to prednisolone sodium phosphate orally disintegrating tablets. Pharmaceutics 13, 1–17. https://doi.org/10.3390/pharmaceutics13010120.

Thomas, J., Stonebrook, E., Kallash, M., 2022. Pediatric hypertension: review of the definition, diagnosis, and initial management. Int J Pediatr Adolesc Med 9, 1–6. https://doi.org/10.1016/j.ijpam.2020.09.005.

Trenfield, S.J., Tan, H.X., Goyanes, A., Wilsdon, D., Rowland, M., Gaisford, S., Basit, A. W., 2020. Non-destructive dose verification of two drugs within 3D printed polyprintlets. Int. J. Pharm. 577, 199066. https://doi.org/10.1016/j.ijpharm.2020.119066.

Uestuener, P., Ferrarini, A., Santi, M., Mardegan, C., Bianchetti, M.G., Simonetti, G.D., Milani, G.P., Lava, S.A.G., 2014. Taste acceptability of pulverized brand-name and generic drugs containing amlodipine or candesartan. Int. J. Pharm. 468, 196–198. https://doi.org/10.1016/j.ijpharm.2014.04.035.

Utkarsh, Hegab, H., Tariq, M., Syed, N.A., Rizvi, G., Pop-Iliev, R., 2020. Towards Analysis and Optimization of Electrospun PVP (Polyvinylpyrrolidone) Nanofibers. Advances in Polymer Technology 2020, 1–9. DOI: 10.1155/2020/4090747.

Vrijens, B., De Geest, S., Hughes, D.A., Przemyslaw, K., Demonceau, J., Ruppar, T., Dobbels, F., Fargher, E., Morrison, V., Lewek, P., Matyjaszczyk, M., Mshelia, C., Clyne, W., Aronson, J.K., Urquhart, J., 2012. A new taxonomy for describing and defining adherence to medications. Br. J. Clin. Pharmacol. 73, 691–705. https://doi.org/10.1111/j.1365-2125.2012.04167.x.

Wildy, M., Lu, P., 2023. Electrospun nanofibers: shaping the future of controlled and responsive drug delivery. Materials 16. https://doi.org/10.3390/ma16227062.

World Health Organization, 2023. Roadmap towards ending TB in children and adolescents.

Wu, Y.H., Yu, D.G., Li, X.Y., Diao, A.H., Illangakoon, U.E., Williams, G.R., 2015. Fast-dissolving sweet sedative nanofiber membranes. J. Mater. Sci. 50, 3604–3613. https://doi.org/10.1007/s10853-015-8921-4.

Zhao, L., Orlu, M., Williams, G.R., 2021. Electrospun fixed dose combination fibers for the treatment of cardiovascular disease. Int. J. Pharm. 599, 120426. https://doi.org/10.1016/j.ijpharm.2021.120426.

Zhou, Y., Wang, M., Yan, C., Liu, H., Yu, D.G., 2022. Advances in the application of electrospun drug-loaded nanofibers in the treatment of oral ulcers. Biomolecules. https://doi.org/10.3390/biom12091254.